

Semiconductor Waveguide Optical Isolator Incorporating Ferromagnetic Epitaxial MnSb for High Temperature Operation

This content has been downloaded from IOPscience. Please scroll down to see the full text.

2008 Appl. Phys. Express 1 022002

(<http://iopscience.iop.org/1882-0786/1/2/022002>)

View [the table of contents for this issue](#), or go to the [journal homepage](#) for more

Download details:

IP Address: 131.112.10.178

This content was downloaded on 19/07/2017 at 16:39

Please note that [terms and conditions apply](#).

You may also be interested in:

[Waveguide-Based 1.5 \$\mu\text{m}\$ Optical Isolator Based on Magneto-Optic Effect in Ferromagnetic MnAs](#)
Tomohiro Amemiya, Hiromasa Shimizu, Pham Nam Hai et al.

[Decrease in Surface States on GaAs Metal-Semiconductor Field-Effect Transistor by High Temperature Operation](#)
Hajime Sasaki, Kazuo Hayashi, Takashi Fujioka et al.

[High Temperature Operation of 5.5 \$\mu\text{m}\$ Strain-Compensated QuantumCascaded Lasers](#)
Lu Xiu-Zhen, Liu Feng-Qi, Liu Jun-Qi et al.
[Thermally Stable Schottky Barrier Diode by Ru/Diamond](#)
Kazuhiro Ikeda, Hitoshi Umezawa, Kumaresan Ramanujam et al.

[Cryocooler operation of SNIS Josephson arrays for AC Voltage standards](#)
A Sosso, N De Leo, M Fretto et al.

[Yttria-Stabilized Zirconia Ceramic Deposition on SS430 Ferritic Steel Grown by PLD - Pulsed Laser Deposition Method](#)
Abu Khalid Rivai, Mardiyanto, Agusutrisno et al.

[Diamond based detectors for high temperature, high radiation environments](#)
A. Metcalfe, G.R. Fern, P.R. Hobson et al.

[The Development of an Intelligent Hybrid Active-passive Vibration Isolator](#)
Changgeng Shuai, Jianguo Ma and Emiliano Rustighi

[Magneto-optical Overcoating of MnSb Films by Surface Oxidation](#)
Hiroyuki Akinaga, Shintaro Miyanishi and Yoshishige Suzuki

Semiconductor Waveguide Optical Isolator Incorporating Ferromagnetic Epitaxial MnSb for High Temperature Operation

Tomohiro Amemiya*, Yusuke Ogawa¹, Hiromasa Shimizu², Hiro MuneKata¹, and Yoshiaki Nakano[†]

Research Center for Advanced Science and Technology, The University of Tokyo, 4-6-1 Komaba, Meguro-ku, Tokyo 153-8904, Japan

¹Imaging Science and Engineering Laboratory, Tokyo Institute of Technology, 4259-G2-13 Nagatsuta, Midori-ku, Yokohama 226-8502, Japan

²Department of Electrical and Electronic Engineering, Tokyo University of Agriculture and Technology, 2-24-16 Nakacho, Koganei, Tokyo 184-8588, Japan

Received November 26, 2007; accepted December 9, 2007; published online January 25, 2008

A 1.5- μm nonreciprocal-loss waveguide optical isolator having improved transverse-magnetic-mode (TM-mode) isolation ratio was developed. The device consisted of an InGaAlAs/InP semiconductor optical amplifier covered with a ferromagnetic epitaxial MnSb layer. Because of the high Curie temperature ($T_c = 314^\circ\text{C}$) and strong magneto-optical effect of MnSb, the nonreciprocal propagation of 11–12 dB/mm has been obtained at least up to 70°C . © 2008 The Japan Society of Applied Physics

DOI: 10.1143/APEX.1.022002

Waveguide optical isolators that can be monolithically integrated with other waveguide devices such as lasers and amplifiers are indispensable for stable operation of photonic integrated circuits (PICs).^{1–6} One promising way of producing waveguide isolators is by making use of *nonreciprocal propagation loss*—a magneto-optical phenomenon where, in an optical waveguide combined with a ferromagnetic layer, the propagation loss of light is larger in backward than in forward propagation. On the basis of theoretical proposals,^{7,8} several experiments have been reported on transverse-electric-mode (TE-mode) and transverse-magnetic-mode (TM-mode) nonreciprocal-loss isolators at 1.3- μm and 1.55- μm telecommunication wavelength bands.^{9–14}

The authors' group first built a TE-mode isolator, consisting of an InGaAsP/InP semiconductor optical-amplifying (SOA) waveguide combined with a ferromagnetic Fe layer,⁹ and obtained an isolation ratio of 14.7 dB/m.¹² Encouraged by this result, we then started developing a TM-mode waveguide isolator. The key to developing the TM isolator is the selection of an appropriate ferromagnetic material because, in a device that operates in TM mode, the ferromagnetic layer is also used as a contact layer for the current injection into the SOA waveguide. Therefore, the ferromagnetic layer has to (i) have a strong magneto-optical effect along with a large saturation magnetization and (ii) provide a low-barrier contact for III–V semiconductors. Ordinary ferromagnetic metals such as Fe and Co are not suited for this purpose because they produce a Schottky barrier on III–V semiconductors resulting in a high contact resistance. In addition, they produce undesirable paramagnetic materials such as FeAs and CoAs at the contact interface and, therefore, degrade the microscopic flatness of the interface.

We previously proposed using manganese–arsenide (MnAs) as the material for the ferromagnetic layer.^{13,14} MnAs is a ferromagnetic intermetallic compound with a nickel–arsenide structure that can be grown epitaxially on GaAs, InP, and related semiconductors.¹⁵ We fabricated a TM-mode device with a MnAs layer and obtained the isolation ratio of 7.2 dB/mm at a wavelength of 1.54 μm . This device was, however, unable to operate at temperatures

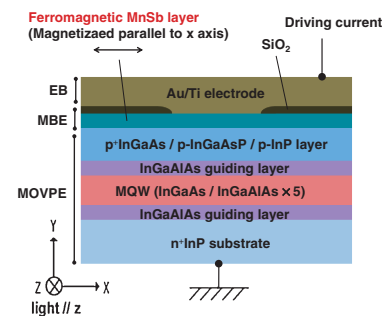


Fig. 1. Schematic cross section of TM-mode waveguide optical isolator with epitaxially-grown ferromagnetic MnSb layer.

higher than room temperature (RT) because the Currie temperature of MnAs is only 40°C . Moreover, the isolation ratio obtained was not large enough for certain applications.

To overcome these problems, in this paper, we have for the first time adopted manganese antimonide MnSb—a ferromagnetic compound with a crystal structure identical to that of MnAs.^{16,17} The Currie temperature of MnSb is 314°C , which is far higher than that of MnAs. In addition, MnSb has a larger value of the off-diagonal element of the dielectric tensor and a larger saturation magnetization than those of MnAs; therefore the effect of the nonreciprocal loss phenomenon was expected to be greater.

Figure 1 schematically shows a cross section, perpendicular to the direction of light propagation, of our TM-mode waveguide isolator at 1.55- μm operation wavelength. The device consists of a TM-mode SOA waveguide covered with a ferromagnetic MnSb layer. The SOA waveguide consists of an InGaAs/InGaAlAs multiple quantum well (MQW) sandwiched between InGaAlAs guiding layers. A ferromagnetic MnSb layer covers the SOA surface, and two interface layers (an InGaAs contact layer and an InGaAsP/InP double cladding layer, colored in light blue in the figure) are inserted between the two. An Au/Ti double metal layer covers the MnSb layer, forming an electrode for current injection into the SOA. Light passes through the SOA waveguide in a direction perpendicular to the figure (z direction).

To operate the device, an external magnetic field is applied as indicated by the arrow in the figure (x direction). The distribution of light in the SOA waveguide extends into

*E-mail address: ametomo@hotaka.t.u-tokyo.ac.jp

†E-mail address: nakano@ee.t.u-tokyo.ac.jp

the MnSb layer to a certain penetration depth and interacts with the magnetized MnSb layer. This produces a difference in complex effective refractive index of TM-polarized light between the forward (+ z) and backward ($-z$) propagation; the propagation loss is larger for backward than forward propagation. This nonreciprocal loss is caused by the magneto-optic transverse Kerr effect. The SOA is operated to compensate for forward propagation loss.

The SOA waveguide structure was grown on a n^+ -InP(100) wafer by the metal-organic vapor phase epitaxy (MOVPE). It was composed of a bottom undoped $\text{In}_{0.53}\text{Ga}_{0.23}\text{Al}_{0.24}\text{As}$ (100-nm thick) guiding layer, a MQW active structure, an upper undoped $\text{In}_{0.53}\text{Ga}_{0.23}\text{Al}_{0.24}\text{As}$ guiding layer (100 nm), a two-layer cladding structure, and a p^+ - $\text{In}_{0.53}\text{Ga}_{0.47}\text{As}$ contact layer (10 nm). The MQW consisted of five undoped $\text{In}_{0.48}\text{Ga}_{0.52}\text{As}$ wells (each 13-nm thick, under 0.4% tensile-strained) and six undoped $\text{In}_{0.62}\text{Ga}_{0.1}\text{Al}_{0.28}\text{As}$ barriers (each 8-nm thick, under 0.6% compressive-strained). Photoluminescence from the MQW showed an emission peak wavelength of 1.54 μm at RT. The cladding layer consisted of a p -InP layer (0.25- μm thick) and a p - $\text{In}_{0.66}\text{Ga}_{0.34}\text{As}_{0.27}\text{P}_{0.73}$ layer (0.15- μm thick, absorption edge = 1.4 μm). This two-layer structure gives a good balance between optical confinement in the SOA waveguide and the extension of light into the MnSb layer.

After the formation of the SOA waveguide, a 160-nm MnSb layer was grown on the surface of the InGaAs contact layer using molecular beam epitaxy (MBE). The wafer was first heated up to 480 $^{\circ}\text{C}$ under an As beam flux in a MBE chamber to remove the native oxide layer on the contact layer. A 20-nm-thick $\text{In}_{0.53}\text{Ga}_{0.47}\text{As}:\text{Be}$ buffer layer was then grown at 450 $^{\circ}\text{C}$. The temperature was then lowered to 250 $^{\circ}\text{C}$, but the supply of the As flux was continued. After that, Mn and Sb fluxes were supplied on the surface to grow a 160-nm MnSb layer at a growth rate of 80 nm/h. The Mn/Sb beam flux ratio was 3.2. The deposition of MnSb was finished with a flat surface, as confirmed by the streaky feature of reflection high-energy electron diffraction (RHEED) patterns. An X-ray diffraction pattern showed strong MnSb peaks in [1011] and [2022] directions and a weak Mn_2Sb peak in the [0004] direction (see Fig. 2). This data showed that hexagonal MnSb(101) was primarily deposited on a InGaAs(100) surface with a small amount of Mn_2Sb coexisting with MnSb as a second phase. Details of the growth process and characterizations of MnSb layers on InGaAs will be reported by Ogawa and others in a different paper.¹⁸⁾

After the growth of the MnSb layer, an SiO_2 layer was deposited on the MnSb layer using magnetron sputtering, and a 2.5- μm -wide stripe window was opened using wet chemical etching. We then used electron-beam evaporation to deposit a 100-nm Ti layer and a 200-nm Au layer on the surface to form an electrode. Figure 3 is a cross section of the device observed with a scanning electron microscope. The MnSb layer showed strong in-plane magneto-crystalline anisotropy and was easily magnetized along the [011] direction of the InP substrate with a saturation magnetization of 850 emu/cm^3 , which was larger than that of MnAs, 600 emu/cm^3 . Therefore, we formed the waveguide stripe parallel to the [011] direction and applied an external magnetic field in the [011] direction (x -direction in Fig. 1).

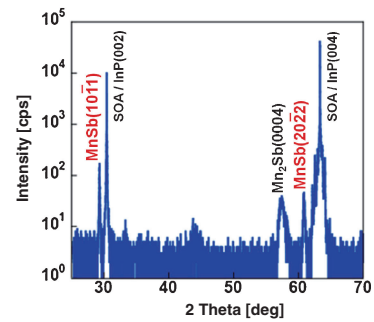


Fig. 2. X-ray diffraction spectrum of the device with epitaxial MnSb layer.

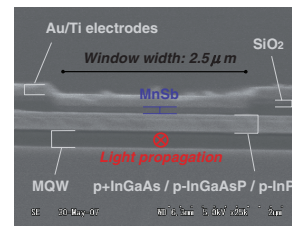


Fig. 3. Cross sectional scanning electron micrograph of the MnSb waveguide optical isolator.

We measured the nonreciprocal transmission of light in the device and demonstrated that the device functioned efficiently as a TM-mode optical isolator at temperatures higher than RT. Our measurement setup consisted of a wavelength-tunable laser with a polarization controller, optical circulators and switches, and an optical spectrum analyzer. The polarization-controlled light from the laser was transferred into and out of the device by lensed fibers. The intensity of incident light and the SOA driving current were set to 5 dBm and 80 mA. The voltage drop across the 0.6 mm-long device was 1.6 V (SOA diode drop 0.9 V plus contact drop 0.7 V), whereas the drop across a reference device with Fe-Ni layers instead of MnSb was 3.0 V (SOA diode drop 0.9 V plus contact drop 2.1 V).¹⁹⁾ This showed the superiority of MnSb over ordinary ferromagnetic metals. While the measurements were being done, the device was magnetized by an external magnetic field of 0.1 T, and temperature was changed between 20 and 70 $^{\circ}\text{C}$ using a thermoelectric cooler.

Figure 4 shows the TM-mode transmission spectra of the device. The wavelength of incident light was fixed at 1.54 μm , the gain peak wavelength of the SOA. The intensity of the output light from the device is plotted as a function of wavelength for forward (blue line) and backward (red line) propagation at temperatures of (a) 20 $^{\circ}\text{C}$ and (b) 70 $^{\circ}\text{C}$. The nonreciprocity, or isolation ratio, at 70 $^{\circ}\text{C}$ was 11.2 dB/mm, which is larger than that of our previous device using MnAs, 7.2 dB/mm at 20 $^{\circ}\text{C}$. The large isolation ratio and high temperature capability are due to the large off-diagonal element and saturation magnetization, as well as the high Currie temperature, of MnSb.

Figure 5 shows the temperature dependence of the isolation ratio and the transmission intensity at 1.54 μm wavelength measured for (a) TM-polarized and (b) TE-polarized light. The device showed nonreciprocity only for

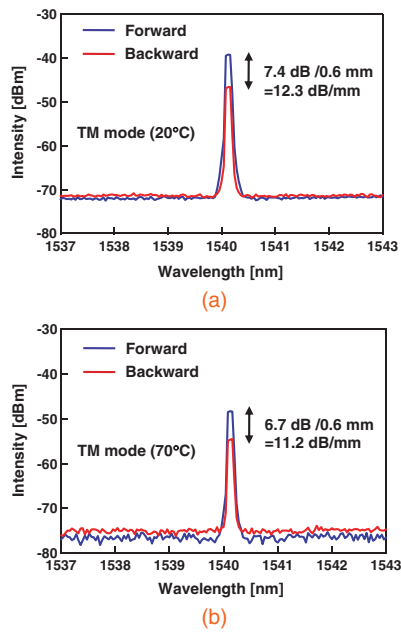


Fig. 4. Typical transmission spectra of the fabricated device for forward (blue line) and backward (red line) propagating 1.54- μm TM-light at temperatures of (a) 20°C and (b) 70°C with 80 mA driving current and with 0.1 T external magnetic field. The device length and the intensity of incident light were 0.6 mm and 5 dBm, respectively.

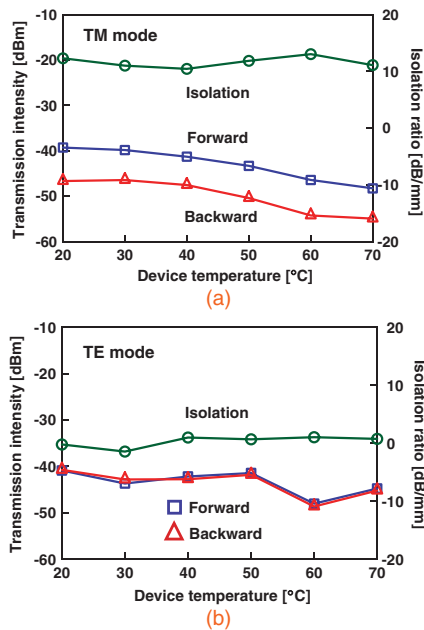


Fig. 5. Transmission intensities at 1.54- μm wavelength as functions of device temperature measured for (a) TM and (b) TE modes, under driving current of 80 mA and external magnetic field of 0.1 T. Derived Isolation ratios are also plotted.

the TM mode. The isolation ratio for the TM mode was 11–12 dB/mm over the temperature range between 20 and 70°C, whereas it was less than 1 dB/mm for the TE mode. The transmission intensity for the TM-polarized light gradually decreased with an increase in temperature, as

shown in Fig. 5(a), because the TM-mode SOA waveguide gain became smaller and its peak shifted towards the longer wavelength side with temperature.

The forward propagation loss observed in this sample device was rather large, as can be seen in Figs. 4 and 5. This was so because the intrinsic propagation loss of the device was still as large as approximately 16 dB at RT after subtracting the loss due to lensed-fiber coupling in the measurement system (12.5 dB/facet \times 2), and the output coupler loss (3 dB). The TM-mode optical gain in the SOA waveguide, approximately 15 dB/mm, was insufficient to compensate the intrinsic propagation loss. We are currently working on two ways to reduce the intrinsic loss of devices. One is to improve the gain in the SOA waveguide by increasing the number of wells in the MQW region. The other is to reduce the propagation loss due to diffraction by incorporating a strong index guiding of a ridge waveguide structure.

In summary, we fabricated a MnSb/InGaAlAs/InP waveguide optical isolator for the first time. The high Curie temperature and strong magneto-optical effect of MnSb produced a large optical isolation of 12 dB/mm at 20°C and 10 dB/mm or greater at 70°C.

Acknowledgment A part of this research (the epitaxial growth of MnSb) was supported by Grants-in-Aid for Scientific Research from the Japan Society for the Promotion of Science (No. 17206002), the Ministry of Education, Culture, Sports, Science and Technology (No. 19048020), and by the National Science Foundation IT program (DMR-0325474).

- 1) J. Fujita, M. Levy, R. M. Osgood, L. Wilkens, and H. Dotsch: *Appl. Phys. Lett.* **76** (2000) 2158.
- 2) H. Yokoi, T. Mizumoto, N. Shinjo, N. Futakuchi, and Y. Nakano: *Appl. Opt.* **39** (2000) 6158.
- 3) M. Levy: *IEEE J. Sel. Top. Quantum Electron.* **8** (2002) 1300.
- 4) S. Y. Sung, X. Qi, and B. J. H. Stadler: *Appl. Phys. Lett.* **87** (2005) 121111.
- 5) T. R. Zaman, X. Guo, and R. J. Ram: *IEEE Photonics Technol. Lett.* **18** (2006) 1359.
- 6) B. M. Holmes and D. C. Hutchings: *Appl. Phys. Lett.* **88** (2006) 061116.
- 7) M. Takenaka and Y. Nakano: *Proc. Int. Conf. Indium Phosphide and Related Materials*, 1999, p. 289.
- 8) W. Zaets and K. Ando: *IEEE Photonics Technol. Lett.* **11** (1999) 1012.
- 9) H. Shimizu and Y. Nakano: *Jpn. J. Appl. Phys.* **43** (2004) L1561.
- 10) M. Vanwolleghem, W. Van Parys, D. Van Thourhout, R. Baets, F. Lelarge, O. Gauthier-Lafaye, B. Thedrez, R. Wrix-Speetjens, and L. Lagae: *Appl. Phys. Lett.* **85** (2004) 3980.
- 11) W. Van Parys, B. Moeyersoon, D. Van Thourhout, R. Baets, M. Vanwolleghem, B. Dagens, J. Decobert, O. Le Gouezigou, D. Make, R. Vanheertum, and L. Lagae: *Appl. Phys. Lett.* **88** (2006) 071115.
- 12) H. Shimizu and Y. Nakano: *J. Lightwave Technol.* **24** (2006) 38.
- 13) T. Amemiya, H. Shimizu, Y. Nakano, P. N. Hai, M. Yokoyama, and M. Tanaka: *Appl. Phys. Lett.* **89** (2006) 021104.
- 14) T. Amemiya, H. Shimizu, P. N. Hai, M. Yokoyama, M. Tanaka, and Y. Nakano: *Appl. Opt.* **46** (2007) 5784.
- 15) M. Tanaka, J. P. Harbison, T. Sands, T. L. Cheeks, and G. M. Rothberg: *J. Vac. Sci. Technol. B* **12** (1994) 1091.
- 16) H. Akinaga, K. Tanaka, K. Ando, and T. Katayama: *J. Cryst. Growth* **150** (1995) 1144.
- 17) S. A. Hatfield and G. R. Bell: *J. Cryst. Growth* **296** (2006) 165.
- 18) Y. Ogawa: in preparation for publication.
- 19) T. Amemiya, H. Shimizu, and Y. Nakano: *Proc. Int. Conf. Indium Phosphide and Related Materials*, 2005, p. 303.